

Comparison of ice-shelf creep flow simulations
with ice-front motion of Filchner-Ronne Ice
Shelf, Antarctica, detected by SAR
interferometry

Christina L Hulbe

Department of the Geophysical Sciences, The University of Chicago
Chicago IL, 60637

Eric Rignot

Jet Propulsion Laboratory, California Institute of Technology
Pasadena, CA, 91109

and

Douglas R. MacAyeal

Department of the Geophysical Sciences, The University of Chicago
Chicago IL, 60637

July 10, 1997

Abstract

Comparison between numerical model ice-shelf flow simulations and synthetic aperture radar (SAR) interferograms is used to study the dynamics at the Hemmen Ice Rise (HIR) and Lassiter Coast (LC) corners of the iceberg-calving front of the Filchner-Ronne Ice Shelf (FRIS). The interferograms are constructed from SAR images provided by European Space Agency's (ESA) Remote Sensing Satellites (ERS 1 and 2). Narrow bands of large shear strain rate are observed along the boundaries between fast-flowing ice shelf ice and no-flow boundaries. Large rifts, opened where the ice shelf separates from the coast, appear to be filled with a melange of sea-ice, ice-shelf fragments, and wind-blown snow. Trial-and-error is used to find the best match between artificial interferograms, constructed from modelled ice flow, and the observed interferograms. We find that at both HIR and LC, ice within the coastal boundary layers must be significantly softer than adjacent ice. At HIR the rift-filling ice melange transmits stress from one ice-shelf fragment to another, thus it must have mechanical competence and must moderate both ice-shelf separation from the coast and the release of icebergs. However, the ice melange along the LC does not. The difference may be related to melange thickness, which could vary in the two locations due to differences in sub-ice shelf oceanography or perhaps to regional atmospheric warming, currently underway along the Antarctic Peninsula. Future warming could weaken the melange ice around HIR as well, causing the ice shelf to loose contact with that shelf-front anchor.

1 Introduction

Understanding the dynamical processes that govern the location of iceberg-calving fronts in the Ross and Weddell seas is a long-standing problem in Antarctic ice-sheet stability and response to climate change. Those processes influence directly the areal extent of the ice sheet and the net heat and salt exchanges between air and sea. It is clear that the mechanical connection between an ice shelf, and the bay walls which confine it and the ice rises and islands which penetrate into it are important in maintaining a stable shelf-front position. That connection is not well-described because extensive crevassing and iceberg calving make field observations of ice shelf margins both difficult and dangerous.

Historical data suggests that calving from large ice shelves is episodic, with long periods of ice-front advance punctuated by short periods of relatively rapid retreat (see for example, Jacobs and others, 1986; Rott and others, 1996). Cyclic behavior suggests that the mean front position depends on internal, glaciological controls such as the rate of ice spreading required to maintain contact with a coast or ice rise, and the formation of large-scale rifts, which separate the ice shelf from its coastal margin and provide the planes of weakness along which tabular icebergs calve. However, correlations between retreat of small ice shelves and southward migration of the -5° C mean-annual atmospheric surface isotherm around the Antarctic Peninsula (Vaughan and Doake, 1996), however, suggest that an external, environmental control may select the mean ice front position. A successful description of ice-shelf front stability must accommodate those two seemingly independent controls on ice-front location, (one an internal glaciological control and the other an external climate control). Here, a resolution is proposed which is based on interferometric observations and finite-element modelling of the separation of the Filchner-Ronne Ice Shelf from Hemmen Ice Rise (HIR) and from the Lassiter Coast (LC).

The HIR and LC corners of the FRIS calving front (Figures 1) illustrate two "classic" types of shelf-front geometries: at HIR the front position appears to be anchored by an intruding ice rise (and by Berkner Island) and along the LC the shelf front diverges from a confining bay wall where it can no longer spread sufficiently to maintain contact with the coast (Sanderson, 1979). Synthetic aperture radar (SAR) images (Figures 2 and 3; from Rignot and MacAyeal, submitted) re-

veal that at both locations, the rifts and coastal separation cavities are filled with what appears to be a melange of multiyear sea ice, ice-shelf fragments, and wind-blown snow. Interferograms constructed by Rignot and MacAyeal (submitted) from these SAR images show that the melange deforms, presumably in response to ice shelf flow. Finite-element models that are tuned to match the interferograms suggest that at HIR, the melange must possess sufficient mechanical strength to influence ice-shelf flow and to maintain some mechanical interaction between the ice shelf and coast after the two have separated. In contrast, the melange along the LC does not appear to influence ice-shelf flow.

The link between “internal” and “external” controls on ice-front location, suggested by the present work, is as follows. Large-scale rifting and coastal separation are processes that occur at a number of locations, all of which may be potential ice-front locations. Rifting and separation in cold environmental conditions fail to introduce an ice front because the melange of multiyear sea ice that fills the voids reconnects the ice shelf across rifts and with the coast. Rifting and separation that do produce an ice front do so because local environmental conditions fail to permit the melange to bind the ice shelf together. Moreover, we suggest that because the thin melange will melt more rapidly than the thicker ice shelf ice, it may facilitate rapid ice-front retreat in future-warming scenarios.

2 Data and Model Description

Ice-shelf flow and tidal motion in the LC area are observed using SAR interferograms derived from 8 passes of the ERS satellites 1 and 2, during their tandem mission in early 1996. A sequence of 7 SAR images from the 1992 ERS 1 “ice phase” mission are used to observe the area around HIR. Both sets of observations are described in Rignot and MacAyeal (submitted). One ascending- and one descending-satellite-pass interferogram, filtered for tidal motion (using the interferogram differencing methods described by Rignot and MacAyeal, submitted), are used for each location.

Interpreting the pattern of ice motion depicted in the interferograms is complicated slightly because the motion is from the perspective of the orbiting satellite, rather than in the horizontal plane or

along an ice flowline. Also, the dynamical implications of ice displacement may not be obvious. We address those limitations by visual comparison between the observations and artificial interferograms that correspond to the satellite look direction of the observations. The artificial interferograms are created using a finite-element numerical model of ice shelf flow in the same area as covered by the interferograms. The model (described in MacAyeal and others, submitted; see also, MacAyeal and others, 1996) computes ice velocity for given ice thicknesses and boundary conditions, using the typical ice-shelf stress-balance equations and assumptions about ice rheology. The finite-element mesh resolution is fine enough to trace rift boundaries and to accommodate narrow boundary layers.

3 Model Sensitivity Experiments

Two series of sensitivity experiments, in which ice softness and melange ice thickness are varied, are used to investigate the importance of coastal boundary layer softening and of the ice melange that fills shelf-front rifts at HIR and along the LC. The cause of ice softening is not specified but it is reasonable to assume some softening due to strain heating and ice crystal alignment (see for example, Echelmeyer and others, 1994; Hulbe and Whillans, in press) will occur within the rapidly shearing margin between fast-flowing ice shelf ice and the adjacent coast. The melange is idealized simply as thin ice, with the same rheologic properties and dynamics and the surrounding ice shelf. Melange thickness will vary, due to ice flow divergence, ice age, and environmental conditions but we do not intend to reproduce the interferograms exactly (as would be possible with a formal inverse method) so that simplification is acceptable. Our goal is to find the best match between observed and artificial interferograms, in order to determine what combination of model parameters best account for the observed dynamical processes.

Four experiments are conducted with the LC model. Experiment 1 assumes no boundary-layer ice softening and has open-water rifts. Experiment 2 assumes a boundary-layer ice softening of 50% (a flow law rate constant of about $1 \times 10^8 \text{ Pa s}^{-1/3}$, reduced from $2 \times 10^8 \text{ Pa s}^{-1/3}$) in a 5 km wide band along the unnamed promontory east of Hansen Inlet, extending downstream in the crevassed wake of the promontory,

and has open-water rifts. Experiment 3 assumes no boundary-layer ice softening and fills the rifts with a 25 m thick ice melange. Experiment 4 assumes a boundary-layer ice softening of 50% and has a melange thickness of 25 m. The HIR experiments are similar to the LC experiments and are described in detail in MacAyeal and others (submitted) so only the LC experiments are presented here.

A qualitative assessment of model performance for the assumptions in each experiment is made by comparing artificial and observed interferograms. We compare fringe spacing and orientation but not absolute velocities so error in the comparisons should be limited to error in the observed interferometric fringes, typically about 1/28th of a fringe (Rignot and MacAyeal, submitted), and error due to unfiltered tidal displacement. The most favorable comparisons for the HIR experiments (Figure 4, from MacAyeal and others, submitted) are obtained with 50% boundary-layer softening and a melange thickness of 10 m. Boundary layer ice softening is required to reproduce the narrow fringe spacing around HIR. The thin, contiguous layer of rift-filling ice must be present to reproduce the observed pattern of fringe spacing within the main ice shelf. The melange ice must, therefore, be mechanically competent enough to transmit stress across rifts and between ice shelf fragments. Comparisons for LC experiments 2 and 3 (Figure 5) demonstrate similarities and differences between the two shelf-front corners. Clearly, experiment 2 provides better matches to the observed interferograms. Softening along the interior margin is important in both locations. However, at LC, the best match is made when the rifts are simulated as being ice-free. The rift-filling melange of ice observed in SAR images and interferograms along the LC does not influence flow in the main ice shelf and must not be a mechanically competent unit. Thus, the melange material is important in binding the rifted shelf front together at HIR but does not appear to have any affect along the LC.

4 Discussion

The comparison between model-derived and observed interferograms presented here demonstrates the dynamical importance of two features common at the corners of ice-shelf fronts. First, coastal boundary-layer ice must be substantially softer than adjacent ice-shelf ice. At

both HIR and the LC, the soft ice is advected downstream into areas where rifting begins (in the wake of HIR in Figure 2 and downstream of Hansen Inlet in Figure 3). Weakness introduced into the ice shelf by that softening may determine where rifting begins and shelf fronts form. That weakness may be opposed by the second feature studied here, the ice melange that fills shelf front rifts and coastal separation cavities. At HIR, the melange provides mechanical coupling across rift walls and between the ice shelf and the adjacent coasts of HIR and Berkner Island. That coupling maintains a connection to Berkner Island farther seaward than horizontal spreading of ice shelf ice would allow and it binds together the rift walls along which large icebergs eventually calve. That "glue" probably allows the shelf front to extend beyond its stable position and prolongs the time before calving occurs.

The ice melange glue may also be the shelf-front's "Achilles Heel", because it would be more vulnerable to melting than thicker ice shelf ice. Indeed, the melange ice observed along the Lassiter Coast offers no such mechanical stability. The reason for that difference in melange competence may reflect a difference in melange thickness or temperature. The LC melange ice could be warmed and melted as high salinity shelf water flows below the ice shelf, along the western boundary of the Weddell Sea (Jacobs and others, 1985). Another tantalizing possibility is that the melange provides the link between shelf-front position, ice dynamics, and climate. Warming due to the southward progression of atmospheric warming observed around the Antarctic Peninsula (Vaughan and Doake, 1996) may be weakening the thin layer of ice. The Lassiter Coast is 3° north of Hemmen Ice Rise and so the ice melange there may respond to regional warming there sooner than at HIR.

An example of the vulnerability of rift-filling ice to regional warming may be the sudden disaggregation of the Larsen-A Ice Shelf in January, 1995 (Rott and others, 1996). The break-up, during a storm, followed several consecutive warm summer seasons. It is possible that water-filled crevasses penetrated the entire thickness of the shelf, creating a network of wounds held together by remaining bridges between crevasses and by frozen sea water within the crevasses — similar to the melange observed here within the LC rifts. The crevasse-filling material, weakened by a particularly warm summer (suggested by extensive melt ponds on the surface of the ice shelf), would have been more vulnerable to failure during a large storm event than the thicker

ice shelf. The atmospheric and sea-surface warming currently underway around the Antarctic Peninsula may progress southward, toward the Antarctic interior. That warming could weaken rift-filling sea-ice melange, making events like those on Larsen A more common around Antarctica.

Acknowledgments

Support for this research was provided by the European Space Agency (ERS-1/2 project code: AO2.USA.160), the National Aeronautics and Space Administration (NASA) of the U.S. (NAGW-5005) and a NASA Graduate Student Fellowship (awarded to C. L. Hulbe). We thank Andrew Gabriel for help in the project inception. David Vaughan, Chris Doake, Richard Frolich and other colleagues at the British Antarctic Survey provided ice-thickness data for the FRIS and many suggestions during the course of the research reported here.

References

- [1] Hulbe, C.L. and I.M. Whillans. in press. Weak bands within ice stream B, West Antarctica, *J. of Glaciol.*
- [2] Jacobs, S.S., R.G. Fairbanks, and Y. Horibe, 1985. Origin and evolution of water masses near the antarctic continental margin: Evidence from $H_2^{18}O/H_2^{16}O$ ratios in seawater, Antarctic Research Series. **43**, 59-85.
- [3] Jacobs, S.S., D. R. MacAyeal and J. L. Ardai, Jr., 1986. The recent advance of the Ross Ice Shelf, Antarctica. *Journal of Glaciology*, **32**(112), 464-474.
- [4] MacAyeal, D. R. , E. Rignot and C. L. Hulbe. 1997. Dynamics of the Filchner-Ronne Ice Shelf Revealed by SAR Interferometry: 2. Model/SAR Intercomparison Involving the Hemmen Ice Rise Flow Regime. For submission to *J. Glaciol.*
- [5] Rignot, E., D. R. MacAyeal, and C.L. Hulbe. 1997. unpublished. Antarctic CRC, 13-18 July 1997.
- [6] Rignot, E., and D. R. MacAyeal. 1997. Dynamics of the Filchner-Ronne Ice Shelf Revealed by SAR Interferometry: 1. Observations of the Ice-Front Calving Margin. For submission to *J. Glaciol.*
- [7] Rott, H., P. Skvarca and T. Nagler, 1996. Rapid collapse of Northern Larsen Ice Shelf, Antarctica. *Science*, **271**, 788-792.
- [8] Peltzer, G., K. W. Hudnut and K. L. Feigl. 1994. Analysis of coseismic surface displacement gradients using radar interferometry: new insights into the Landers earthquake, *J. Geophys. Res.* **99**(B11), 21,971-21,981.
- [9] Sanderson, T.J.O., 1979. Equilibrium profile of ice shelves. *Journal of Glaciology*, **22**(88), 435-60.
- [10] Vaughan, D. G. and C. S. M. Doake, 1996. Recent atmospheric warming and retreat of ice shelves on the Antarctic Peninsula. *Nature*, **379**, 328-331.

Figures

Figure 1. Sketch map of the Filchener-Ronne Ice Shelf. Grounded ice and ice-free rock are shaded grey. Rectangles around the Lasiter Coast and Hemmen Ice Rise areas indicate the locations of SAR images used in this study (shown in Figures 2 and 3).

Figure 2. SAR amplitude images and sketch maps (from Rignot and MacAyeal, submitted), indicating prominent features in the Hemmen Ice Rise area. Descending satellite pass images are in the left-hand column and ascending pass images are in the right-hand column. North is indicated by the arrow labelled N and the satellite look direction is indicated by the arrow labelled R. Several features stand out in the HIR and LC (Figure 3) images: radar-bright bands that indicate extreme crevassing due to shear along coastal boundaries; rifts generated where the sheared ice is advected downstream, in the wake of the unnamed promontory east of Hansen Inlet along the LC and in the wake of HIR; and the melange of sea-ice and in-blown snow that fills rifts in both locations.

Figure 3. SAR amplitude images and sketch maps (from Rignot and MacAyeal, submitted), indicating prominent features in the Lasiter Coast area. Image arrangement is as in Figure 2.

Figure 4. The most favorable HIR experiment results and observed interferograms (from MacAyeal and others, submitted). Descending satellite pass images are in the left-hand column and ascending pass images are in the right-hand column.

Figure 5. Artificial and observed interferograms for the LC experiments. Image arrangement is as in Figure 4. The best match between artificial and observed interferograms is for experiment 2, where a 50% boundary-layer softening is applied and open-water rifts are assumed. The observed interferograms are from Rignot and MacAyeal (submitted).

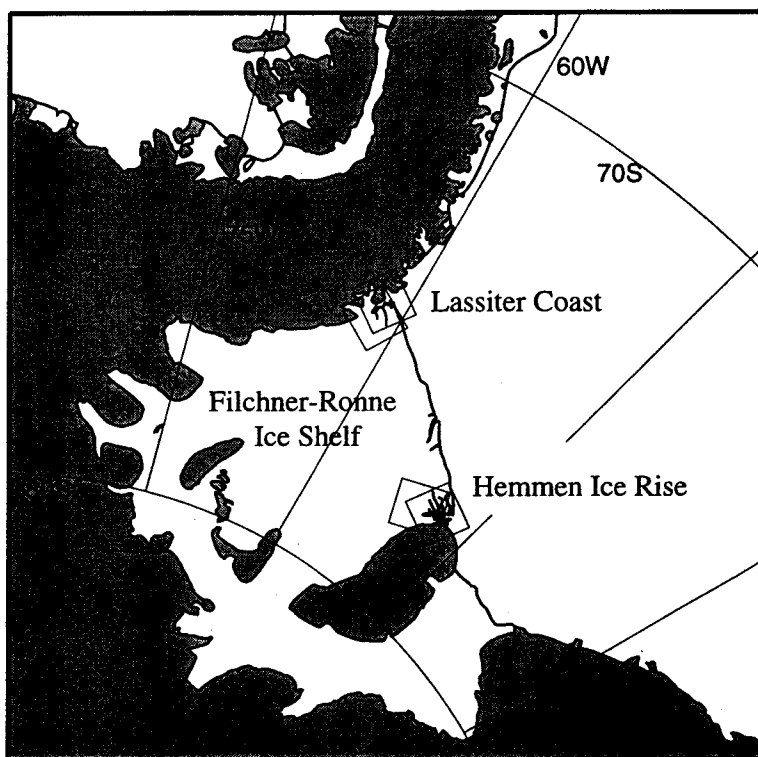


Figure 1

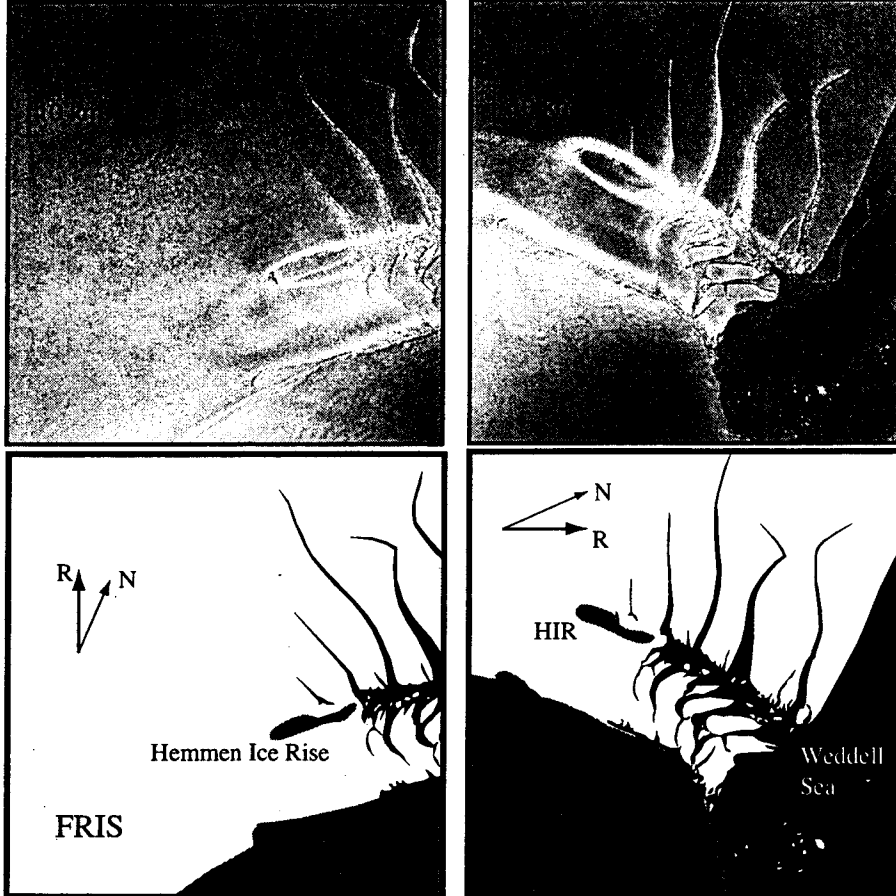


Figure 2

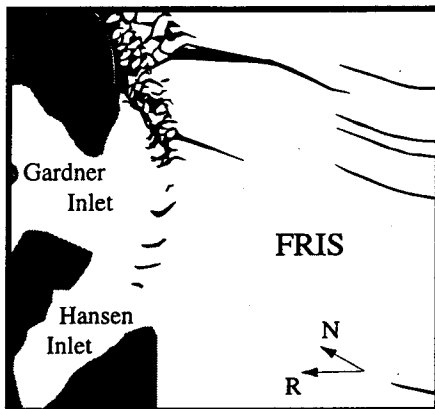
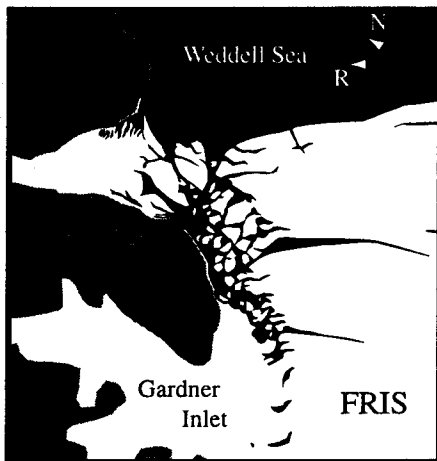
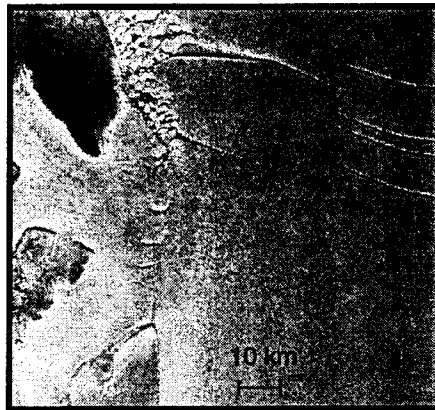
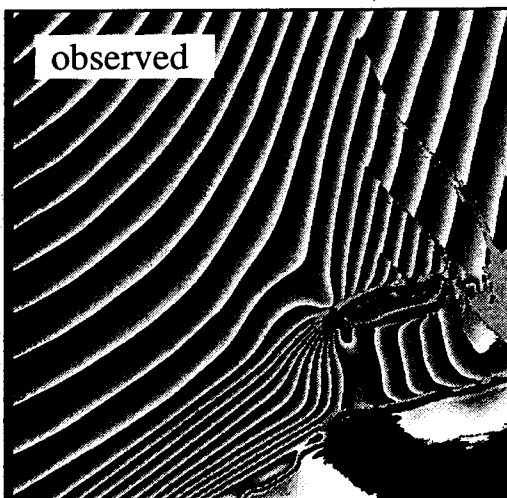
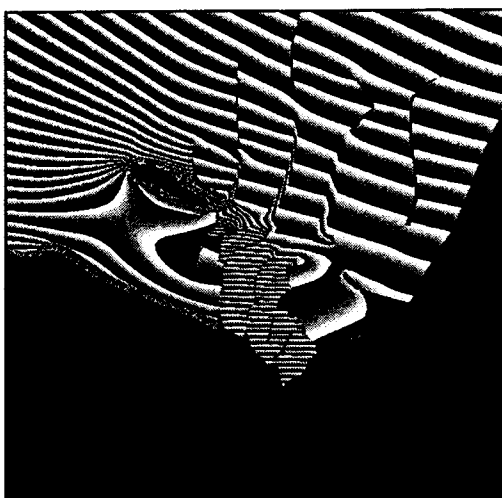
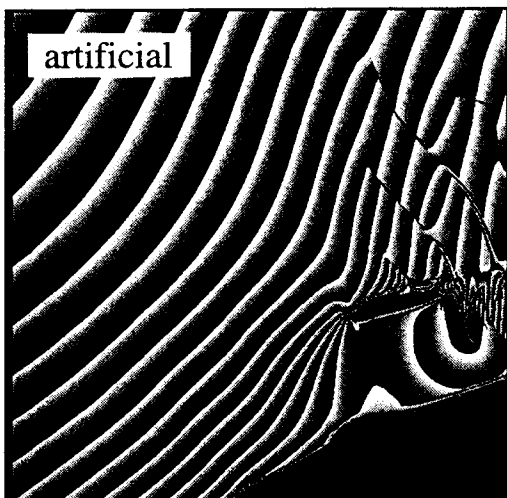
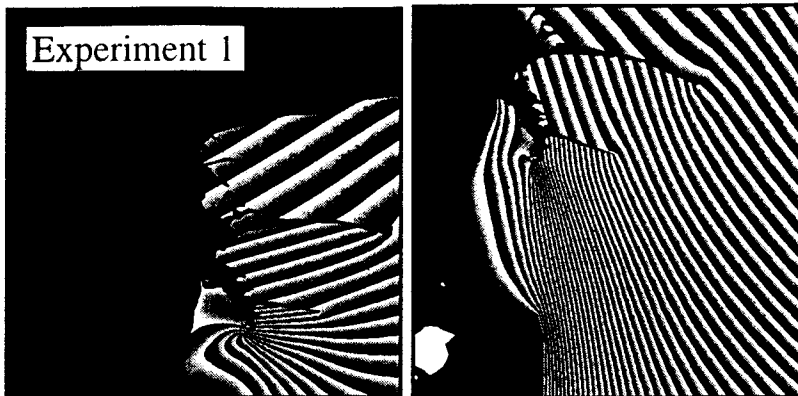


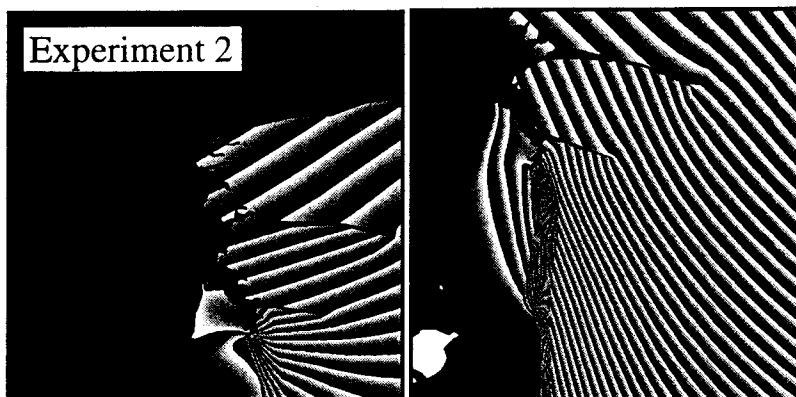
Figure 2



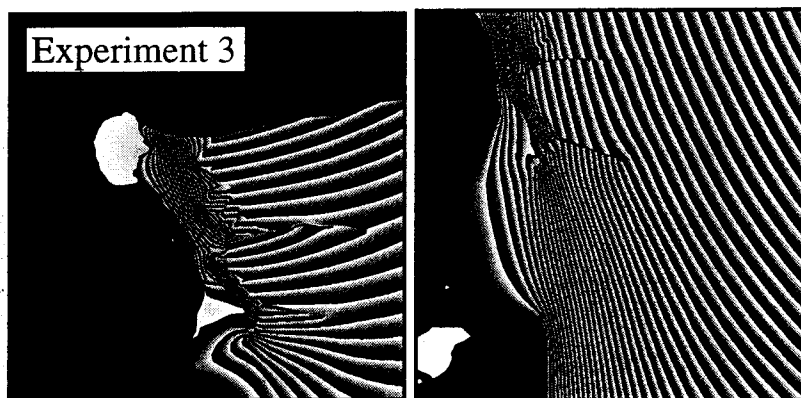
Experiment 1



Experiment 2



Experiment 3



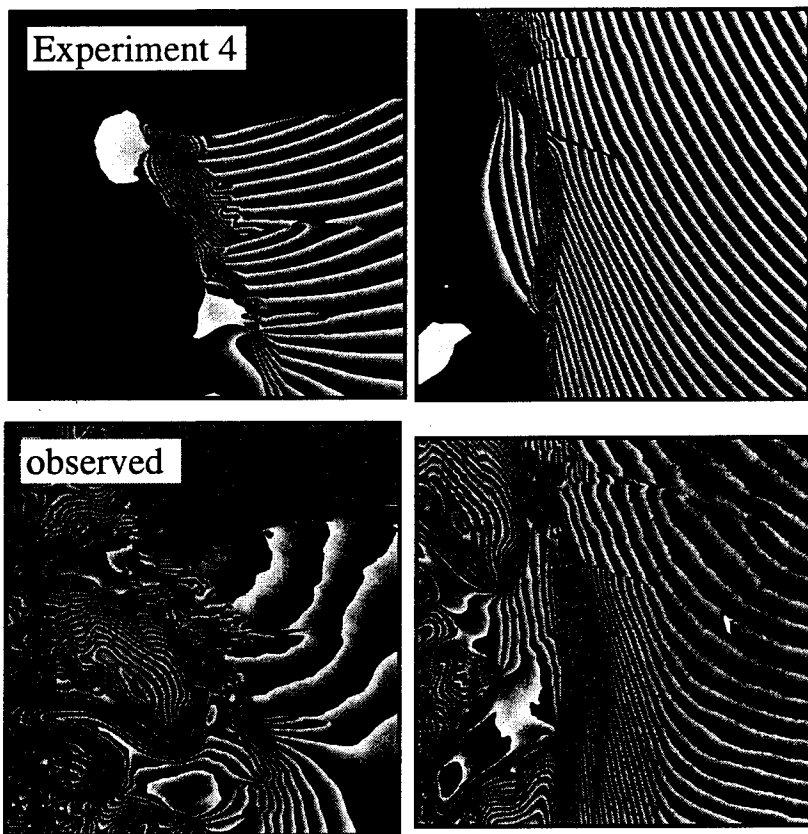


Figure 5 cont.